ER-α36 knockdown is associated with lysosomal dysfunction and proliferation inhibition in liver cancer cells

HUANHUAN HE[1,2*], XUAN WANG[1,2*], ZHIXUAN WEI[1*], AN WANG[1,2], XIANGYUE FANG[1], HANBO HE[1], ZHUORUI WU[1], XIJI SHU[1,3,4], BINLIAN SUN[2-4], QIONGXIA CHEN[1], XUAN HUANG[1], HONGYAN ZHOU[1,3,4], YUCHEN LIU[2-4] and ZHENGQI FU[1,2]

[1]Department of Pathology and Pathophysiology, School of Medicine, Jianghan University, Wuhan, Hubei 430056, P.R. China; [2]Cancer Institute, School of Medicine, Jianghan University, Wuhan, Hubei 430056, P.R. China; [3]Hubei Key Laboratory of Cognitive and Affective Disorders, Jianghan University, Wuhan, Hubei 430056, P.R. China; [4]Wuhan Institute of Biomedical Sciences, School of Medicine, Jianghan University, Wuhan, Hubei 430056, P.R. China

Received February 16, 2025; Accepted July 4, 2025

DOI: 10.3892/mmr.2025.13649

Abstract. Estrogen receptor (ER)-α36 and autophagy have each independently been reported to promote the proliferation of liver cancer cells; however, the association between them has not been explored. Therefore, the present study aimed to investigate the role and the underlying mechanism of ER-α36 in the regulation of autophagy in liver cancer cells. The proliferation of liver cancer cell variants was examined by colony formation assay. A xenograft tumor model in nude mice was used to examine the role of ER-α36 in malignant proliferation of liver cancer cells *in vivo*. Autophagic flux and lysosomal localization were assessed with immunofluorescence and confocal microscopy. The levels of ER-α36, LAMP1, AKT, p62 and LC3-II/I in liver cancer cell variants, and tumors formed by HepG2 cell variants in the nude mice were examined using Western blot and immunohistochemistry. The results revealed that ER-α36 knockdown impaired autophagic flux by increasing lysosomal membrane permeabilization (LMP) and blocking lysosomal degradation. ER-α36 knockdown also significantly inhibited the proliferation of liver cancer cells and orthotopic liver xenograft tumors. In addition, decreased AKT phosphorylation and the juxtanuclear clustering of lysosomes were observed in the liver cancer cells with ER-α36 knockdown. *In vitro* experiments using the AKT inhibitor MK-2206 indicated that AKT is involved in the ER-α36 knockdown-induced changes in LMP and lysosomal localization in liver cancer cells. In summary, the present study revealed that ER-α36 plays a role in regulating the autophagy and proliferation of liver cancer cells, which is associated with the modulation of AKT signaling, LMP and lysosome localization. These findings highlight an important role of ER-α36 in liver tumorigenesis.

Correspondence to: Professor Yuchen Liu, Wuhan Institute of Biomedical Sciences, School of Medicine, Jianghan University, J12 Teaching Building, 8 Sanjiaohu Road, Wuhan, Hubei 430056, P.R. China
E-mail: yuchen.liu@jhun.edu.cn

Professor Zhengqi Fu, Department of Pathology and Pathophysiology, School of Medicine, Jianghan University, J12 Teaching Building, 8 Sanjiaohu Road, Wuhan, Hubei 430056, P.R. China
E-mail: lilyfzq@163.com

*Contributed equally

Key words: estrogen receptor-α36, AKT, lysosomal membrane permeabilization, lysosomal degradation, liver cancer cells

Introduction

Liver cancer is one of the most prevalent and life-threatening cancer types worldwide. Due to its high incidence and global mortality rates, as well as the limited therapeutic options at advanced stages, liver cancer remains a major clinical challenge (1-3).

Estrogen receptor (ER)-mediated signaling is known to contribute to the pathogenesis of liver cancer (4,5). ER-α36, an isoform of ER-α, has been reported to play a critical role in the development of numerous tumors, including liver cancer (6,7). ER-α36 is transcribed from a promoter located in the first intron of the classic ER-α gene. Unlike classical ER-α, ER-α36 is mainly localized on the plasma membrane, where it mediates rapid estrogen signaling (8). ER-α36 expression in primary liver cancer is upregulated compared with that in adjacent non-tumor tissues, contrasting with the expression pattern of classical ER-α (7,9). In addition, ER-α36-mediated rapid estrogen signaling has been shown to promote the growth of PLC/PRF/5 and HepG2 liver cancer cells, in culture and in tumorspheres, through the epidermal growth factor receptor/Src/extracellular signal-regulated kinase axis (10). Tamoxifen, an ER-α antagonist, has not provided survival benefits in patients with breast cancer (11), and ER-α36 has been indicated to contribute to tamoxifen resistance in breast cancer and glioblastoma cells (11,12). These findings suggest that ER-α36, rather than classical ER-α, is the key ER isoform involved in the development and progression of liver cancer.

However, the mechanism underlying the potential contribution of ER-α36 to liver tumorigenesis remains unclear.

Autophagy is a catabolic pathway that maintains cellular homeostasis and supports organelle renewal by removing misfolded proteins, cytotoxic aggregates and damaged organelles (13). During this process, cytoplasmic components are sequestered into autophagosomes, which subsequently fuse with lysosomes to form autolysosomes. Within autolysosomes, cellular contents, including protein substrates, receptors and other autophagosome-associated proteins, are degraded by lysosomal acidic hydrolases (14). Thus, lysosomes function as the terminal degradation component of the autophagic process. Studies have shown that lysosomal dysfunction, including lysosomal membrane permeabilization (LMP), loss of acidity, changes in lysosome localization and defects in lysosome-associated signaling molecules (15-18), can impair the degradative capacity of the lysosomal-autophagy pathway. These dysfunctions have profound implications for the development and progression of numerous diseases, including cancer (19). Tumor cells rely heavily on increased lysosomal function to meet their proliferation and metabolism requirements, which renders them particularly sensitive to lysosomal dysregulation (20,21). For example, it has been found that the re-localization of lysosomes to the tumor cell periphery facilitates the exocytosis of cathepsins, neuraminidase-1 and heparinase, thereby promoting tumor cell invasion, metastasis and angiogenesis (20,22). In addition, lysosomal acidity has been shown to influence cell growth through the maintenance of iron homeostasis (23). Thus, the lysosome is an important regulatory hub for multiple pathways involved in cell proliferation (21). However, the exact mechanism by which lysosomal function contributes to the proliferation of liver cancer cells remains unclear.

In the present study, the role of ER-α36 in regulating the malignant proliferation of liver cancer cells was investigated *in vivo* and *in vitro*. In addition, the role of ER-α36 in autophagy and lysosomal distribution was examined.

Materials and methods

Chemicals and antibodies. 17β-estradiol (E2) was purchased from Sigma-Aldrich; Merck KGaA. The ER-α36 antibody was kindly provided by Dr Zhaoyi Wang (Shenogen Pharma Group). Antibodies against p62 (also known as sequestosome 1; cat. no. 18420-1-AP), galectin-3 (Gal-3; cat. no. 60207-1-Ig), lysosome-associated membrane protein 1 (LAMP1; cat. no. 21997-1-AP), AKT (cat. no. 10176-2-AP), phosphorylated-(p-)AKT (cat. no. 66444-1-Ig) and β-actin (cat. no. 60008-1-IG) were purchased from Proteintech Group, Inc. The microtubule-associated protein 1 light chain 3b (LC3B) antibody (cat. no. A19665) was purchased from ABclonal Biotech Co., Ltd. Antibodies for ubiquitin (Ub; cat. no. AF0306) were purchased from Beyotime Biotech Inc. The Ki67 antibody (cat. no. bs-2130R) was purchased from Biosynthesis Biotechnology Co., Ltd. Chloroquine (CQ; cat. no. HY-17589A) and the AKT inhibitor MK-2206 (cat. no. HY-108232) were obtained from MedChemExpress.

Cell culture, stably transfected cell line preparation and cell treatment. The HepG2 (cat. no. STCC10114) and Huh7 (cat. no. STCC10102) human liver cancer cell lines, which endogenously express ER-α36, were obtained from Shenogen Pharma Group (7). The authenticity of both cell lines was confirmed by STR analysis. The cells were maintained in DMEM (Thermo Fisher Scientific, Inc.) with 10% FBS; Zhejiang Tianhang Biotechnology Co., Ltd.) at 37˚C in a humidified incubator with 5% CO_2.

Stable ER-α36 knockdown cell lines and control cell lines were established as previously described (10,24). In brief, short hairpin RNA (shRNA) targeting human ER-α36 was constructed using the pRNAT-U6.1/Neo vector (provided by Dr Zhaoyi Wang) (25,26). The construct was validated by DNA sequencing. The target sequence was as follows: shER-α36: 5'-GTTCAGTACCTATTGGCA-3' (nucleotides 4,261-4,278; sequence ID: BX640939.1). The empty vector and ER-α36 shRNA expression vector (2 μg/ml) were transfected into the liver cancer cells for 6 h at 37˚C, using Lipofectamine® 2000 (Invitrogen; Thermo Fisher Scientific, Inc.) as the transfection reagent. The transfected cells were selected with 600 μg/ml G418 (Beyotime Institute of Biotechnology) for 3 weeks. After this, cells from ≥25 clones were pooled. The empty vector transfected cells were named HepG2/Vector and Huh7/Vector, and those transfected with ER-α36 shRNA were named HepG2/Sh36 and Huh7/Sh36.

For treatment, the cells were maintained in phenol red-free DMEM with 1% charcoal-stripped fetal calf serum (FCS; Zhejiang Tianhang Biotechnology Co., Ltd.) for 48 h, and then treated with MK-2206 (100 nM) for 6 h, followed by E2 (1 nM) for either 30 min (detection of the phosphorylation levels of AKT) or 24 h (detection of LAMP1 expression) at 37˚C in an atmosphere containing 5% CO_2 (10). An equal volume of alcohol was used as the vehicle control. The cells were treated with CQ (20 μM) for 24 h at 37˚C; the same volume of DMSO was used as the vehicle control.

Western blot analysis. Cells and liver tissues were lysed with RIPA lysis buffer (Beyotime Institute of Biotechnology). Protein concentrations were measured using a BCA Protein Assay Kit. The proteins (20 μg/lane) were separated by 10% sodium dodecyl sulfate-polyacrylamide gel electrophoresis, transferred to polyvinylidene fluoride membranes. The membranes were blocked with 5% skim milk powder in Tris-buffered saline containing 0.1% Tween-20 (TBST) for 1 h at room temperature. After blocking, membranes were incubated overnight at 4˚C with primary antibodies: anti-ER-a36 (1:1,000), anti-LC3B (1:1,000), anti-p62 (1:1,000), anti-Ub (1:1,000), anti-LAMP1 (1:1,000), anti-p-AKT (1:1,000), anti-AKT (1:1,000) and anti-β-actin (1:2,000). After washing with TBST, the membranes were incubated with HRP Conjugated AffiniPure Goat Anti-rabbit/mouse IgG (H + L) secondary antibodies (cat. no. BA1055/BA1051, 1:5,000, Wuhan Boster Biological Technology CO., LTD.) at room temperature for 1 h. Following incubation, membranes were washed in TBST. The target proteins were detected using enhanced chemiluminescence (ECL) detection reagent (BeyoECL Moon kit; Beyotime Institute of Biotech Inc.). Signal intensities were captured using ECL western-blotting analysis system (GE Healthcare). And quantitative analysis was performed using ImageJ version 1.53t software (National Institutes of Health).

Colony formation assay. After seeding ($2x10^3$ cells/well), cells were treated with MK-2206 (100 nM) for 6 h alone or in combination with E2 (1 nM) for 24 h and cultured for 2 weeks at 37˚C. The cell colonies were washed with PBS and fixed with 4% paraformaldehyde for 15 min at 37˚C. After washing with PBS, cells were stained with 1% crystal violet for 30 min at 37˚C. Colonies containing >50 cells were counted. Colonies count was performed using ImageJ v 2.14.0 (FIJI) software (National Institutes of Health).

Immunofluorescence (IF) staining. After seeding ($5x10^3$ cells/well), the cells were fixed in 4% paraformaldehyde for 15 min at room temperature. The tumor tissue was fixed in 4% paraformaldehyde for 24 h at room temperature, dehydrated in graded ethanol, embedded in paraffin, and sectioned into 4 μm slices. After paraffin was removed with xylene at room temperature, the slides were gradually hydrated using ethanol. The slides were incubated in 3% hydrogen peroxide/methanol buffer to quench endogenous peroxidase activity. Antigen retrieval was performed by immersing the slides in ethylenediamine tetra acetic acid buffer (pH 8.0) and boiling for 5 min. Then, the samples were blocked with 5% BSA (BioFroxx) for 1 h at room temperature, incubated with primary antibodies: anti-LC3B (1:500), anti-p62 (1:500), anti-LAMP1 (1:500) and anti-Gal-3 (1:500) overnight at 4˚C, followed by incubation with secondary antibodies conjugated to fluorescein: ABflo® 488-conjugated Goat anti-mouse/rabbit IgG (H+L) (cat. no. AS076/AS053, 1:200, ABclonal Biotech Co.) or ABflo® 594-conjugated Goat anti-mouse/rabbit IgG (H+L) (cat. no. AS054/AS039, 1:200, ABclonal Biotech Co.) for 1 h at room temperature. The nuclei were stained with Hoechst 33342 for 10 min at room temperature. Images were captured using a Leica TCS SP8 confocal microscope (Leica Microsystems. Inc.), and image analysis was performed using ImageJ v 2.14.0 (FIJI) software (National Institutes of Health).

pmCherry-enhanced green fluorescence protein (EGFP)-LC3 puncta assay. After seeding ($1x10^4$ cells/well), cells were infected with the pmCherry-EGFP-LC3b adenovirus (MOI: 20; Beyotime Biotech Inc.) for 12 h at 37 ˚C. Then, the infection medium was replaced with fresh complete medium and cells were cultured for 24 h at 37 ˚C. The nuclei were stained with Hoechst 33342 for 10 min at room temperature. Images were captured using a Leica TCS SP8 confocal microscope (Leica Microsystems. Inc.), and image analysis was performed using ImageJ v 2.14.0 (FIJI) software (National Institutes of Health).

Lyso-Tracker Red staining. After seeding ($5x10^3$ cells/well), cells were incubated in Lyso-Tracker Red (50 nM, Beyotime Institute of Biotech Inc.) for 15 min at 37 ˚C. The nuclei were stained with Hoechst 33342 for 10 min at room temperature, and images were captured using an Olympus BX53 fluorescence microscope (Olympus Co., Ltd).

Animal experiments. All experimental procedures were performed in compliance with the National Institutes of Health guidelines for the Care and Use of Laboratory Animals and approved by the Ethics Committee of Jianghan University (Wuhan, China; approval no. JHDXLL2024-086). A total of 10 male BALB/c-nu mice (5 weeks old, 16-18 g) were purchased from Sipeifu (Beijing) Animal Technology Co., Ltd., and housed in specific pathogen-free conditions at a temperature of 24±2˚C and relative humidity of 60%. The mice were exposed to a 12-h light/dark cycle, and were given free access to mouse feed sterilized and water sterilized by autoclaving. The HepG2/Sh36 and HepG2/Vector cells ($5x10^6$ cells/mouse) were injected into the livers of BALB/c-nu mice (n=4/group) to establish 28-day orthotopic liver xenograft tumor models. The mice were monitored daily for food and water intake, weight, body posture, behavior, distress and response to external stimuli. Several humane endpoints were established, including a >20% loss of body weight, severe dehydration, refusal of food, severe pain or distress, or a moribund state. However, no mice were humanely sacrificed or found dead prior to the designated end of the study. After 28 days, the mice were anesthetized with an intraperitoneal injection of pentobarbital sodium at a dose of 50 mg/kg body weight and sacrificed by cervical dislocation. Death was confirmed when no breathing or heartbeat was detected for >5 min. The livers were then harvested from the mice for further investigation.

H&E Staining. The tumor tissue was fixed in 4% paraformaldehyde for 24 h at room temperature, dehydrated in graded ethanol, embedded in paraffin, and sectioned into 4 μm slices. After paraffin was removed with xylene at room temperature, the slides were gradually hydrated using ethanol. The slides were dyed with hematoxylin for 30 sec at room temperature and eosin for 1 min at room temperature. Images were captured using a light microscope.

Immunohistochemistry (IHC) assay. The tumor tissue was fixed in 4% paraformaldehyde for 24 h at room temperature, dehydrated in graded ethanol, embedded in paraffin, and sectioned into 4 μm slices. After paraffin was removed with xylene at room temperature, the slides were gradually hydrated using ethanol. The slides were incubated in 3% hydrogen peroxide/methanol buffer to quench endogenous peroxidase activity. Antigen retrieval was performed by immersing the slides in ethylenediamine tetra acetic acid buffer (pH 8.0) and boiling for 5 min. The slides were blocked with 5% BSA (BioFroxx) for 1 h at room temperature, incubated with primary antibodies: anti-LC3B (1:200), anti-p62 (1:200), anti-LAMP1 (1:200) and anti-Ki67 (1:200) overnight at 4˚C, followed by incubation with secondary antibodies (goat anti-rabbit/mouse HRP-labeled polymer; cat. no. PV-9000, Beijing Zhong Shan-Golden Bridge Biological Technology CO., Ltd.) for 1 h at 37˚C. The slides were stained with 3,3'-Diaminobenzidine tetrahydrochloride (Beijing Zhong Shan -Golden Bridge Biological Technology CO., Ltd.) and counterstained with hematoxylin for 30 s at room temperature to visualize the cell nuclei. Then, the slides were photographed by a light microscope. Quantification of the positive staining was performed by measuring the integral optical density using ImageJ v 2.14.0 (FIJI) software (National Institutes of Health), with normalization to the stained area.

Statistical analysis. Data are presented as the mean ± standard error of mean of at least three independent experiments. The data were analyzed using GraphPad Prism 8.0 software

(Dotmatics) with one-way analysis of variance (ANOVA) followed by Bonferroni's post hoc tests. $P<0.05$ was considered to indicate a statistically significant difference.

Results

ER-α36 knockdown attenuates the proliferation of liver cancer cells and promotes the accumulation of autophagosomes. To test the role of ER-α36 in the proliferation and autophagy of liver cancer cells, HepG2/Sh36 and Huh7/Sh36 cells were prepared by transfection with an ER-α36 specific shRNA expression vector, and HepG2/Vector and Huh7/Vector control cells were prepared by transfection with an empty expression vector. The successful knockdown of ER-α36 expression was verified by western blotting (Fig. 1A and B). The results of the colony formation assay revealed that ER-α36 knockdown attenuated the colony-forming ability of the liver cancer cells (Fig. 1C and D). The knockdown of ER-α36 expression also increased the LC3-II/LC3-I ratio as revealed by western blot analysis (Fig. 1E and F), and increased the number of LC3-II puncta as shown by IF staining (Fig. 1G). These findings suggest that ER-α36 knockdown promoted autophagosome formation in the liver cancer cells.

ER-α36 knockdown blocks autophagic flux and autophagic degradation. The effect of ER-α36 knockdown on autophagic flux was assessed. Western blotting revealed that the expression of p62, a marker of autophagic flux, was increased in the HepG2/Sh36 and Huh7/Sh36 cells compared with that in the respective empty vector-transfected cells, suggesting that ER-α36 downregulation impaired autophagic flux (Fig. 2A and B). The transfected liver cancer cells were co-transfected with pmCherry-EGFP-LC3b to monitor autophagy. In this system, autophagosomes appear as yellow puncta, due to a combination of GFP and mCherry fluorescence, whereas autolysosomes, formed by autophagosome-lysosomal fusion, are identified by mCherry red fluorescence only. This occurs because when autophagosomes fuse with lysosomes, GFP is quenched by the acidic environment, whereas mCherry remains fluorescent. The liver cancer cells with ER-α36 knockdown exhibited significantly increased numbers of yellow puncta, indicative of autophagosomes, with occasional red dots representing autolysosomes, suggesting that ER-α36 knockdown blocked autophagic flux, thereby resulting in the accumulation of autophagosomes (Fig. 2C and D). Additionally, when the autophagosome-lysosome fusion inhibitor CQ was used to treat the cells, western blotting revealed that ER-α36 knockdown increased the LC3-II/LC3-I ratio in the absence of CQ, but caused no further increase in the presence of CQ. This suggests that ER-α36 knockdown increased the LC3-II/LC3-I ratio due to impaired autophagosome degradation (Fig. 2E and F). Furthermore, ER-α36 downregulation led to the accumulation of ubiquitinated proteins, suggesting that substrate degradation was inhibited (Fig. 2G and H). Taken together, these findings indicate that ER-α36 knockdown impaired autophagic flux by inhibiting the degradation of autophagosomes.

ER-α36 knockdown induces lysosomal damage and LMP. To determine whether the autophagic degradation defect induced by ER-α36 knockdown was due to impaired autophagosome-lysosome fusion or defective lysosomal degradation, IF staining of LC3 (green) and LAMP1 (red) was performed to assess their co-localization (yellow) in liver cancer cells with different levels of ER-α36 expression. Fewer red LAMP1 puncta and yellow co-localization signals were observed in the HepG2/Sh36 and Huh7/Sh36 cells compared with those in the corresponding vector control cells (Fig. 3A), suggesting that ER-α36 knockdown blocked autophagosome-lysosome fusion, thereby contributing to the impairment of autophagic flux in liver cancer cells.

Since lysosomal dysfunction can lead to autophagic flux blockage and the accumulation of lysosomal substrates (27), lysosomal integrity was examined. A significant reduction in the Lyso-Tracker-staining of lysosomes was observed in the HepG2/Sh36 and Huh7/Sh36 cells compared with those in the respective vector control cells (Fig. 3B), suggesting that ER-α36 downregulation compromised the acidic environment within lysosomes. An increase in the pH of the lysosomal lumen is a known indicator of LMP (28). As shown in Fig. 3C, IF staining revealed prominent Gal-3 puncta in the HepG2/Sh36 and Huh7/Sh36 cells, whereas they were only faintly visible in the vector control cells. In addition, western blotting revealed that LAMP1 expression in the HepG2/Sh36 and Huh7/Sh36 cells was decreased compared with that in the vector control cells (Fig. 3D and E). These data indicate that ER-α36 knockdown disrupted lysosomal integrity.

ER-α36 knockdown suppresses the malignant proliferation of liver cancer cells and induces LMP. To investigate the function of ER-α36 in the malignant proliferation of liver cancer cells *in vivo*, nude mice were intrahepatically injected with HepG2/Vector cells or HepG2/Sh36 cells to establish an orthotopic liver xenograft tumor model for 28 days. While tumors were formed in the livers of all mice, the tumor volumes formed by the HepG2/Sh36 cells were significantly smaller than those formed by the HepG2/Vector cells. The liver weight, body weight and ratio of liver weight to body weight exhibited no significant differences between the two groups (Fig. 4A and B). Furthermore, a reduced number of pathological karyomitoses and Ki67-positive cells were detected in the tumors formed from the HepG2/Sh36 cells by H&E and IHC, suggesting that ER-α36 is involved in the malignant proliferation of HepG2 cells (Fig. 4C and D). Western blot analysis and IHC also revealed an increased LC3-II/I ratio and p62 expression level, and decreased LAMP1 expression in the tumor tissues formed by the HepG2/Sh36 cells compared with those in the tumors formed by the HepG2/Vector cells (Fig. 4D, F and G). In addition, IF staining demonstrated an increase in the number of Gal-3 puncta in the tumors formed by the HepG2/Sh36 cells compared with those formed by the HepG2/Vector cells (Fig. 4E). These results indicate that ER-α36 knockdown suppressed the tumor proliferation of HepG2 cells and induced LMP *in vivo*.

ER-α36 knockdown decreases AKT phosphorylation and influences lysosomal localization in liver cancer cells. AKT signaling, a typical event in ER-α36-mediated rapid estrogenic signaling, has been reported to influence lysosomal localization (10,29). To determine whether ER-α36 mediated AKT activation is involved in the regulation of lysosomal

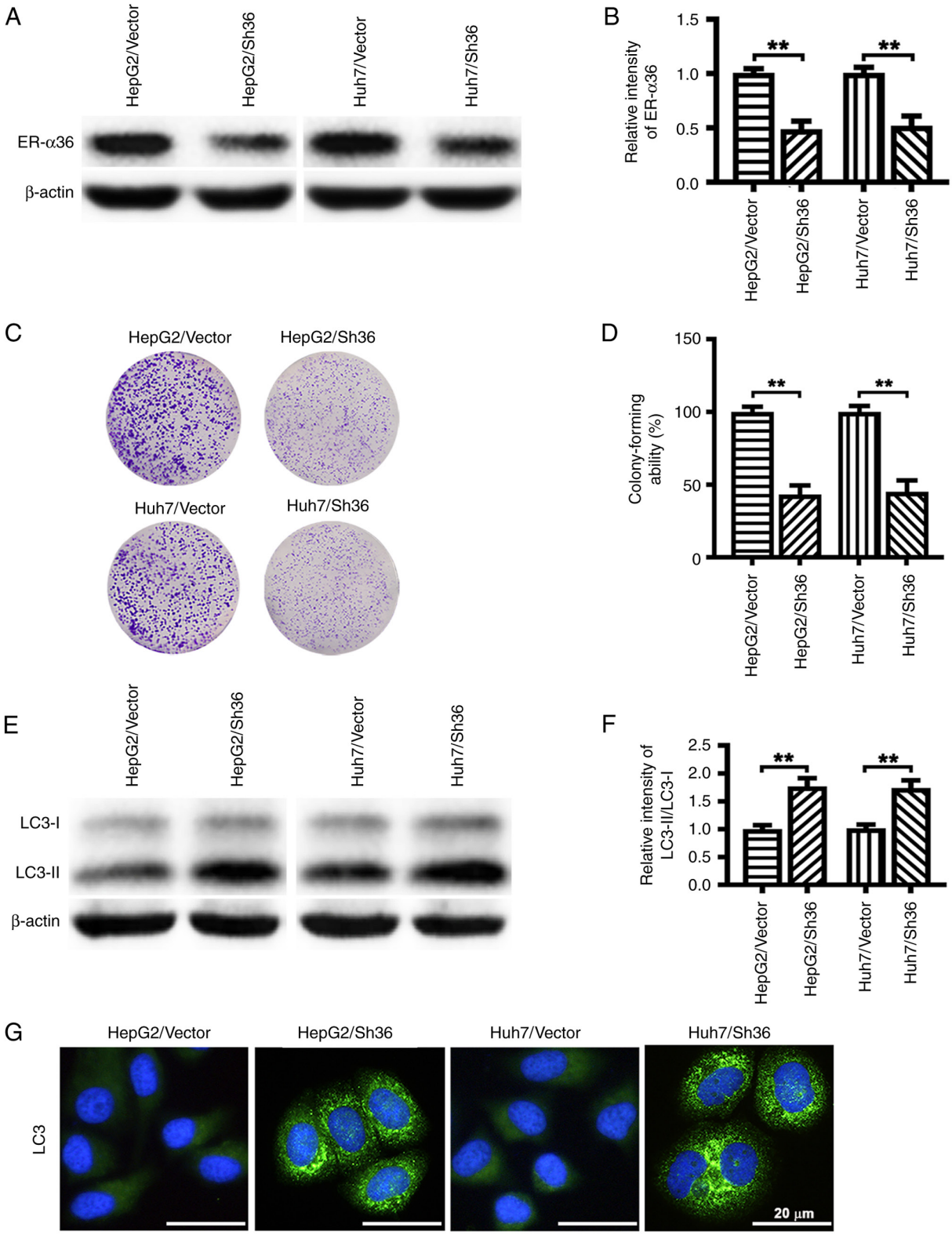

Figure 1. ER-α36 knockdown attenuates the colony formation of liver cancer cells and promotes the accumulation of autophagosomes. Expression of ER-α36 in stably transfected HepG2 and Huh7 cells: (A) Representative western blots and (B) quantitative analysis. (C) Representative images of colony formation by the liver cancer cell variants and (D) quantitative analysis. (E) Levels of LC3-II and LC3-I in the liver cancer cell variants measured by western blotting and (F) quantitative analysis of the LC3-II/LC3-I ratio. Data are presented as the mean ± SEM (n=3). **P<0.01. (G) Analysis of the liver cancer cells by immunofluorescence assay using an LC3 antibody and nuclear staining with Hoechst 33342. Scale bar, 20 μm. ER, estrogen receptor; LC3, microtubule-associated protein 1 light chain 3; Sh36, transfected with ER-α36 specific short hairpin RNA expression vector; Vector, transfected with empty vector.

localization in liver cancer cells, the phosphorylation levels of AKT in the HepG2 and Huh7 cells with and without ER-α36 knockdown and in the tumors formed from them were examined. Decreased AKT phosphorylation at Ser 473 was observed in the liver cancer cells with ER-α36 knockdown and in the tumors formed from them compared with that in

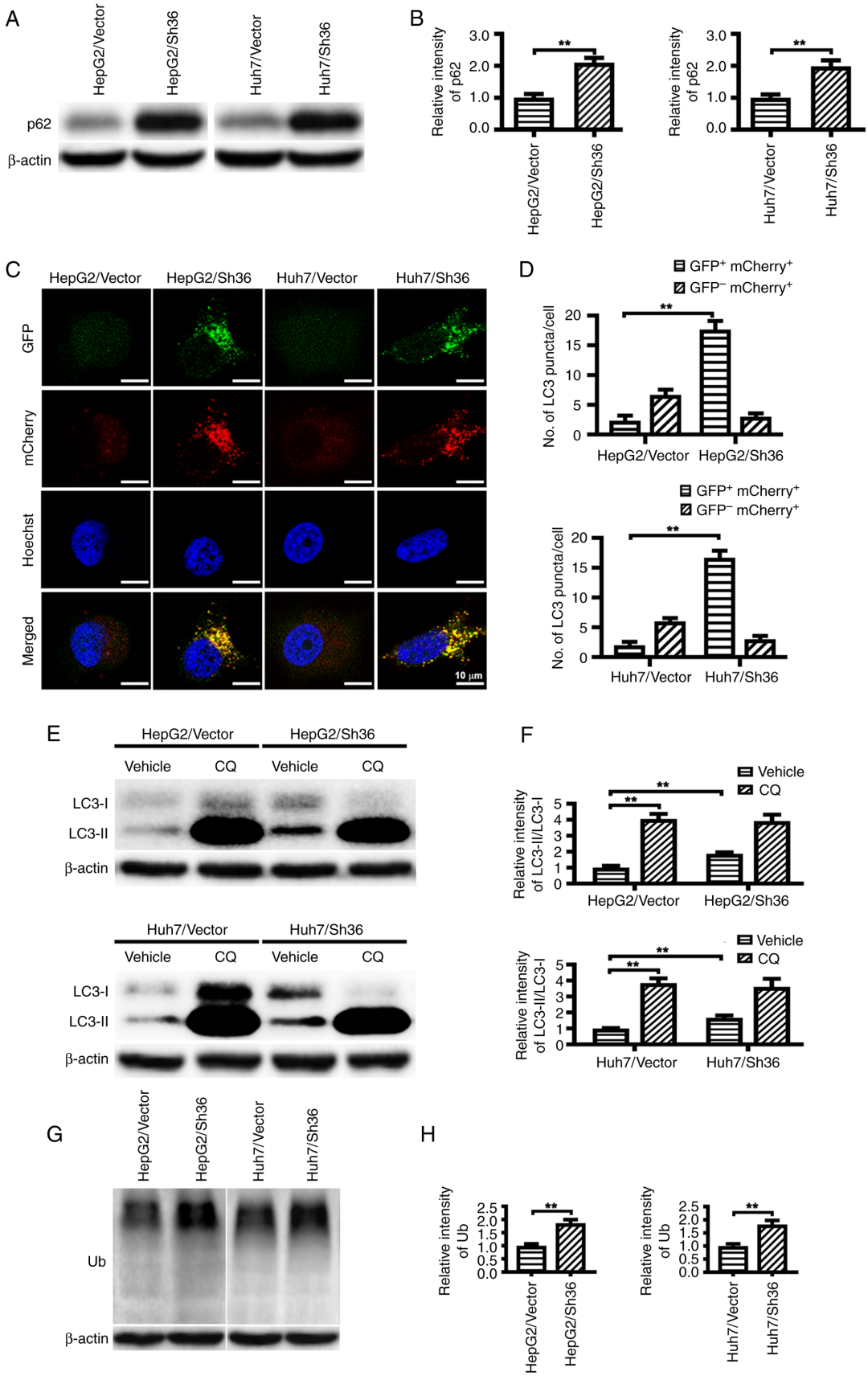

Figure 2. ER-α36 knockdown blocks autophagic flux and degradation. Expression of p62 in stably transfected liver cancer cells with different levels of ER-α36 expression: (A) Representative western blots and (B) quantitative analysis. (C) Confocal microscopy images of liver cancer cells with and without ER-α36 knockdown infected with pmCherry-enhanced GFP-LC3b adenovirus (scale bar, 10 μm) and (D) quantification of yellow and red puncta. (E) Levels of LC3-II and LC3-I assessed by western blotting in transfected liver cancer cells treated with or without CQ (20 μM) for 24 h, and (F) quantitative analysis of the LC3-II/LC3-I ratio. (G) Western blots of ubiquitinated proteins in the transfected liver cancer cells and (H) quantitative analysis of Ub levels. **P<0.01. ER, estrogen receptor; GFP, green fluorescence protein; LC3, microtubule-associated protein 1 light chain 3; CQ, chloroquine; Ub, ubiquitin; Sh36, transfected with ER-α36 specific short hairpin RNA expression vector; Vector, transfected with empty vector.

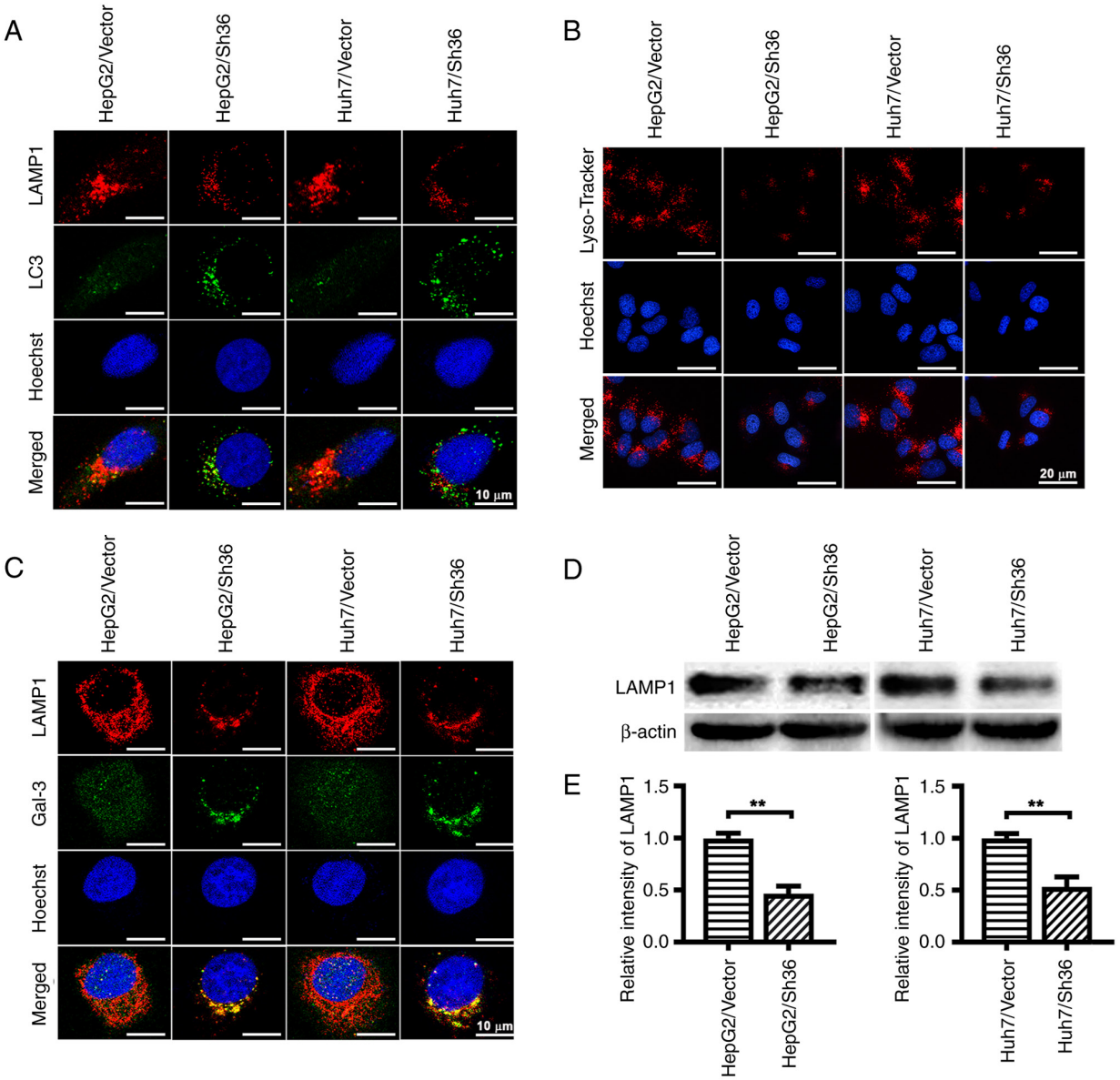

Figure 3. ER-α36 knockdown induces lysosomal damage and membrane permeabilization. (A) Co-localization of LC3 (green) and LAMP1 (red) in stably transfected liver cancer cells with different levels of ER-α36 expression. Scale bar, 10 μm. (B) Fluorescence images of the transfected liver cancer cells following staining with Lyso-Tracker Red. Scale bar, 20 μm. (C) Co-localization of Gal-3 and LAMP1 in the transfected liver cancer cells. Scale bar, 10 μm. (D) Expression levels of LAMP1 in the liver cancer cells evaluated by western blotting and (E) quantitative analysis. Data are presented as the mean ± SEM. **P<0.01. ER, estrogen receptor; LC3, microtubule-associated protein 1 light chain 3; LAMP1, lysosome-associated membrane protein 1; Gal-3, galectin-3; Sh36, transfected with ER-α36 specific short hairpin RNA expression vector; Vector, transfected with empty vector.

the corresponding vector controls (Figs. 4F and G, 5A and B). In addition, when compared with the HepG2/Vector and Huh7/Vector cells, an accumulation of LAMP1 was observed at the juxtanuclear region in the HepG2/Sh36 and Huh7/Sh36 cells (Fig. 5C and D), consistent with earlier reports that the AKT inhibitor MK-2206 promotes the juxtanuclear clustering of lysosomes (29). However, in the present study, MK-2206 did not further reduce AKT phosphorylation or influence lysosome localization in HepG2/Sh36 and Huh7/Sih6 cells (Fig. 5C and D). These results indicate that ER-α36 expression knockdown attenuated AKT phosphorylation, which then led to the juxtanuclear clustering of lysosomes.

AKT is involved in the ER-α36 knockdown-induced changes in lysosomal localization and LMP in liver cancer cells. To examine the effect of AKT on ER-α36 regulated LMP and lysosomal localization, which influence the proliferation of liver cancer cells, the transfected liver cancer cells were treated with E2 and/or MK-2206. It was observed that treatment of the HepG2/Vector and Huh7/Vector cells with E2 upregulated AKT phosphorylation at Ser 473 and increased the colony-forming ability of the cells, and these effects were abrogated by MK-2206 (Fig. 6A, B, E and F). This is consistent with the previous finding that AKT signaling is involved in ER-α36-mediated rapid estrogenic signaling and stimulation of cell proliferation (10). The E2 treatment also upregulated LAMP1 expression (Fig. 6C, D and H), increased Lyso-Tracker fluorescence intensity (Fig. 6G) and re-localized lysosomes to the cell periphery in the HepG2/Vector and Huh7/Vector cells (Fig. 6G), while MK-2206 abrogated all these E2-induced

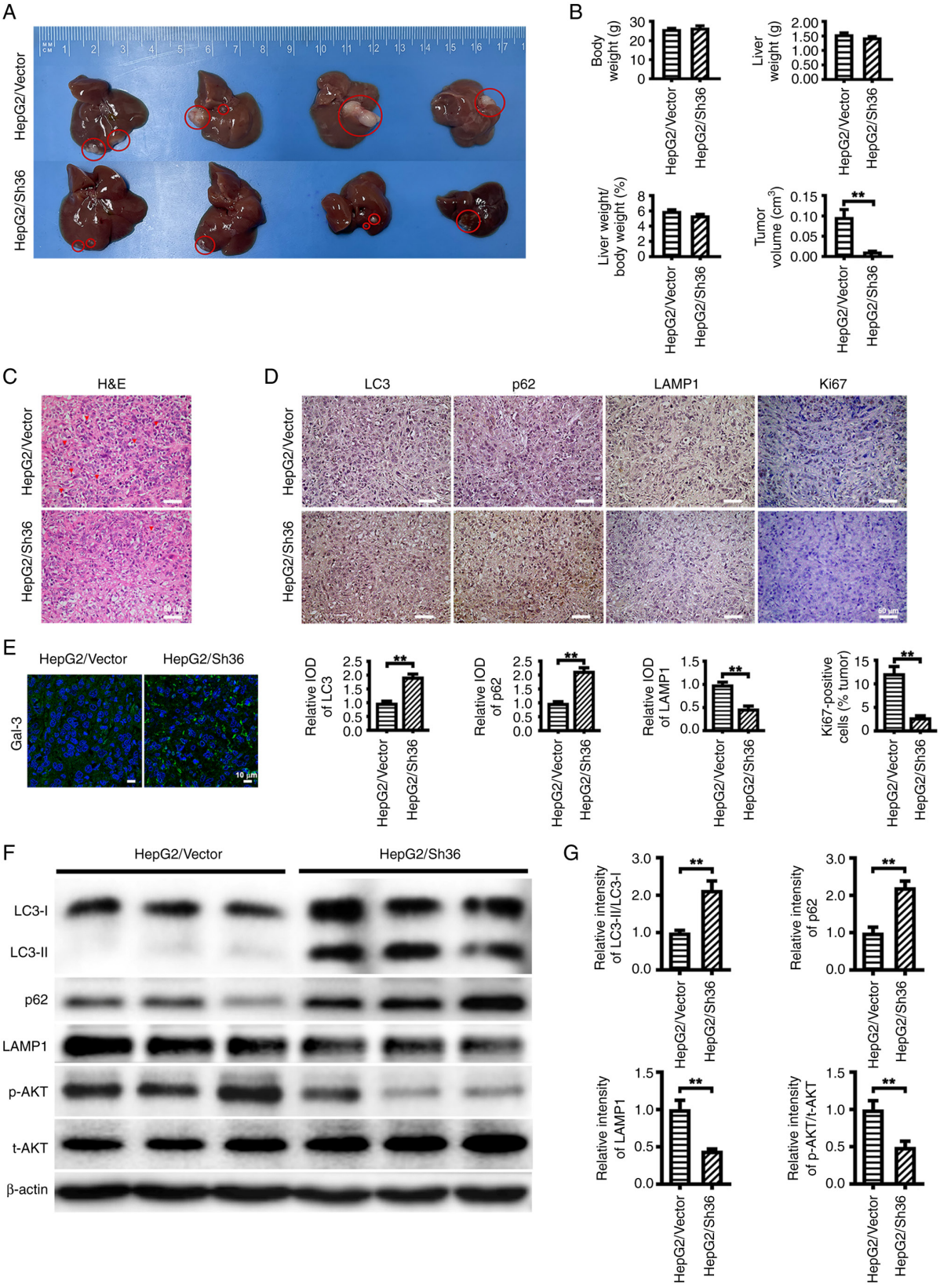

Figure 4. ER-α36 knockdown suppresses the malignant proliferation of liver cancer cells and induces lysosomal membrane permeabilization. (A) Representative images of liver tumors from nude mice intrahepatically injected with HepG2 cells expressing different ER-α36 levels, harvested at 28 days post-injection. (B) Quantitative analysis of liver tumor volume, liver weight, body weight and the ratio of liver weight to body weight. (C) Representative H&E staining images showing pathological karyomitosis changes. Scale bar, 50 μm. (D) Immunohistochemical staining of LC3, p62, LAMP1 and Ki67 with corresponding IOD values. Scale bar, 50 μm. (E) Immunofluorescence staining of Gal-3 in the tumors formed from the transfected HepG2 cells. Scale bar, 10 μm. (F) Western blotting results showing the levels of LC3-II and LC3-II, p62, LAMP1, p-AKT and t-AKT in the tumors, and (G) quantitative analyses of the LC3-II/LC3-I and p-AKT/t-AKT ratios, and p62 and LAMP1 expression levels. β-actin was used as the internal loading control. Data are presented as the mean ± SEM. **P<0.01. ER, estrogen receptor; H&E, hematoxylin and eosin; LC3, microtubule-associated protein 1 light chain 3; LAMP1, lysosome-associated membrane protein 1; Gal-3, galectin-3; IOD, integrated optical density; p-, phosphorylated; t-, total; Sh36, transfected with ER-α36 specific short hairpin RNA expression vector; Vector, transfected with empty vector.

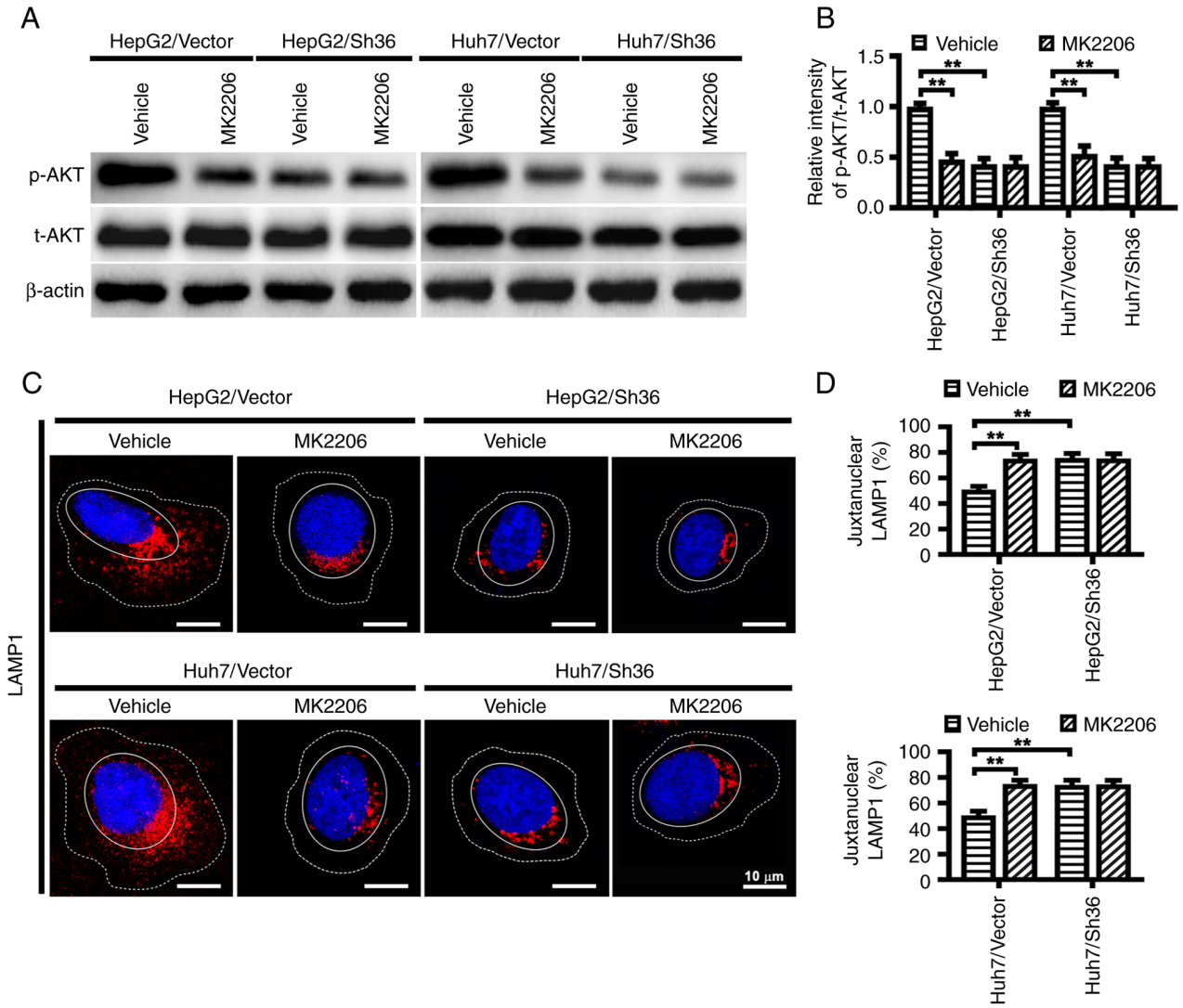

Figure 5. ER-α36 knockdown decreases AKT phosphorylation and influences lysosomal localization in liver cancer cells. Stably transfected liver cancer cells with different levels of ER-α36 expression were treated with or without MK-2206 (100 nM) for 6 h. (A) Representative western blots of p-AKT and t-AKT, and (B) quantitative analysis. (C) Immunofluorescence analysis of LAMP1. Cell peripheries and the juxtanuclear region are indicated with dashed lines and solid lines, respectively. Scale bar, 10 μm. (D) Quantification of the juxtanuclear percentage of LAMP1. **P<0.01. ER, estrogen receptor; p-, phosphorylated; t-, total; LAMP1, lysosome-associated membrane protein 1; Sh36, transfected with ER-α36 specific short hairpin RNA expression vector; Vector, transfected with empty vector.

effects. In addition, a diffuse distribution of Gal-3 in the cytoplasm and nucleus was observed in E2-treated HepG2/Vector and Huh7/Vector cells, while a punctate pattern was observed in the HepG2/Vector and Huh7/Vector cells treated with the combination of E2 and MK-2206 (Fig. 6H). By contrast, these phenomena were almost undetectable in the HepG2/Sh36 and Huh7/Sh36 cells. These findings strongly suggest that AKT is involved in the lysosomal localization and LMP changes associated with ER-α36 knockdown.

Discussion

The present study provides evidence that the knockdown of ER-α36 impaired autophagic flux and inhibited the malignant proliferation of HepG2 and Huh7 human liver cancer cells *in vivo* and *in vitro*. ER-α36 knockdown also induced LMP as well as lysosomal dysfunction, including pH elevation, impaired protein degradation and the juxtanuclear clustering of lysosomes. These findings suggest that the maintenance of normal lysosomal function is one of the key roles of ER-α36 in liver cancer cells.

Previous studies have suggested that ER-α36 is involved in liver tumorigenesis (10), that ER-α36 mRNA levels gradually increase from normal liver tissue to cirrhotic liver and liver carcinoma tissues (7), and that upregulated ER-α36 expression is associated with primary liver cancer (9). In addition, the knockdown of ER-α36 expression has been shown to attenuate the metastasis of HepG2 and Huh7 cells by downregulating epithelial-mesenchymal transition and the Src signaling pathway (24). Furthermore, ER-α36 has been demonstrated to be a prognostic factor in breast cancer (30). However, the molecular mechanism by which ER-α36 promotes cancer cell proliferation is unclear.

Impaired autophagy has been linked to various pathological conditions in humans, including liver dysfunction and carcinogenesis (31). In glioblastoma cells, ER-α36 has been reported to counteract tamoxifen-mediated cell apoptosis by

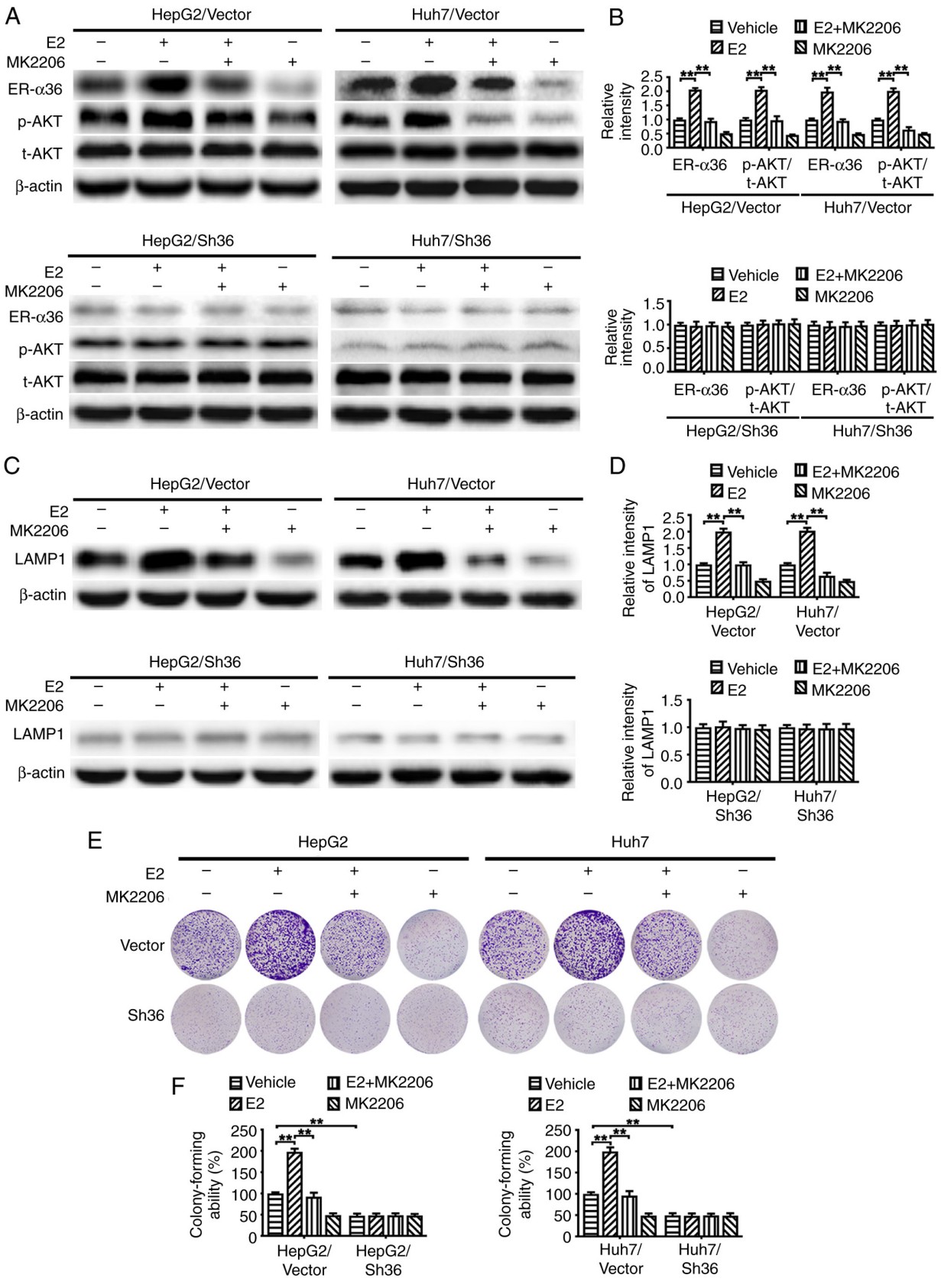

Figure 6. Continued.

promoting autophagy via inactivation of the AKT/mammalian target of rapamycin (mTOR) signaling pathway (12). Furthermore, ER-α36 promotes autophagy during the development of acquired tamoxifen resistance (12,32), and its expression level has been shown to correlate with that of p62 in a three-dimensional culture model (12).

The present study also demonstrated that ER-α36 knockdown attenuated the malignant proliferation of liver cancer

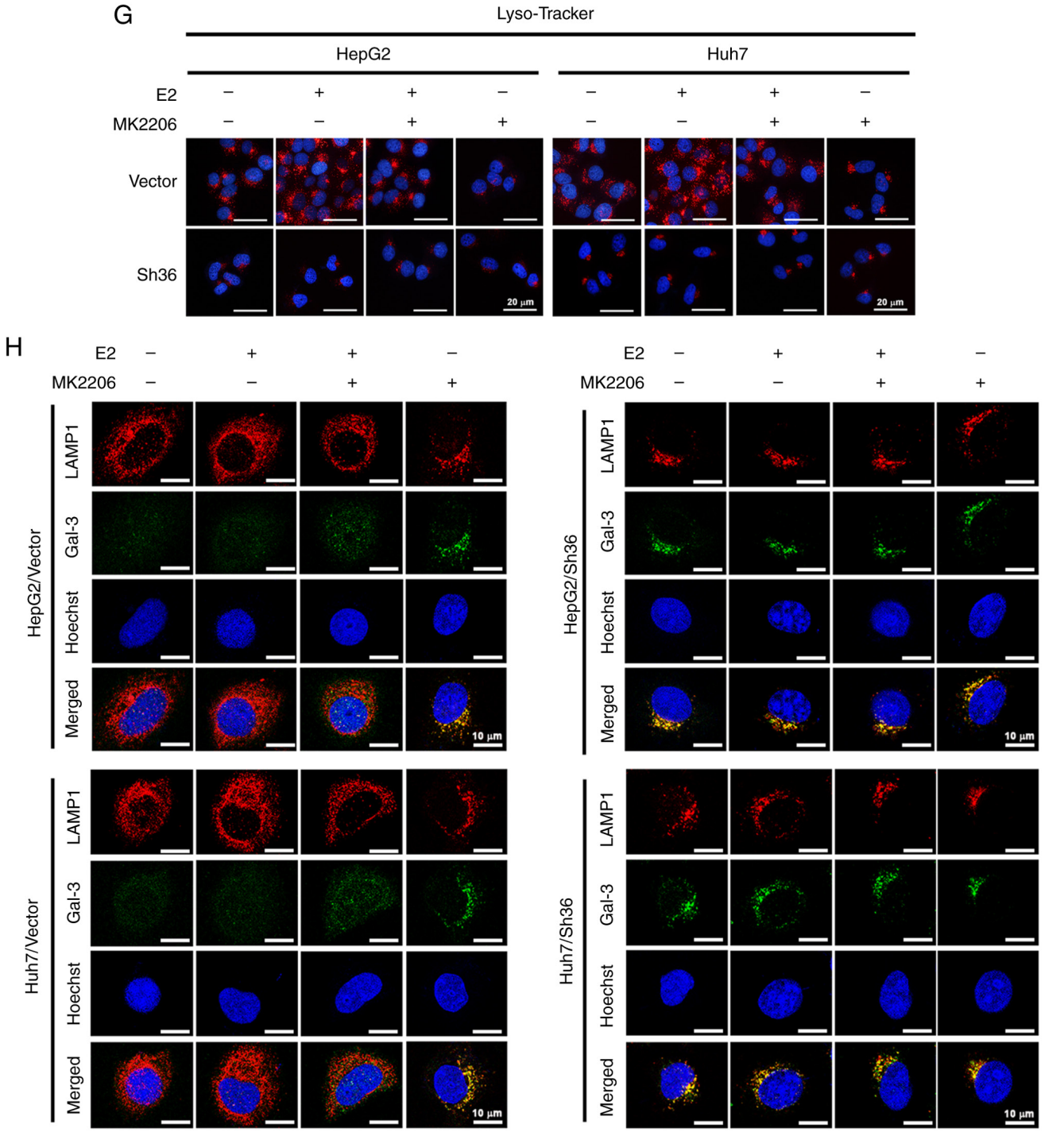

Figure 6. AKT is involved in the lysosomal localization and LMP induced by ER-α36 knockdown. Transfected liver cancer cells with different levels of ER-α36 expression were treated with MK-2206 (100 nM) for 6 h, followed by E2 (1 nM) for 30 min, and the same volume of alcohol was used as a vehicle control. (A) Representative western blots of ER-α36, p-AKT and AKT, and (B) quantitative analysis of ER-α36 expression and the p-AKT/t-AKT ratio. In subsequent assays, the transfected liver cancer cells were treated with MK-2206 (100 nM) for 6 h, followed by E2 (1 nM) for 24 h. (C) Representative western blots of LAMP1 and (D) quantitative analysis of LAMP1 expression. (E) Representative images of colony formation by the liver cancer cells and (F) quantitative analysis of colony forming ability. Data are presented as the mean ± SEM. **P<0.01. (G) Fluorescence microscopy images of the cells following staining with Lyso-Tracker Red. Scale bar, 20 μm. (H) Co-localization of Gal-3 (green) and LAMP1 (red) in the cells as revealed by immunofluorescence staining. Scale bar, 10 μm. ER, estrogen receptor; E2, 17β-estradiol; Gal-3, galectin-3; p-, phosphorylated; t-, total; LAMP1, lysosome-associated membrane protein 1; Sh36, transfected with ER-α36 specific short hairpin RNA expression vector; Vector, transfected with empty vector.

cells and impaired autophagic flux. Specifically, ER-α36 knockdown increased the LC3-II/LC3-I ratio and p62 expression levels in HepG2 and Huh7 cells, as well as in the tumor tissues formed by these cells in mice, compared with those in the corresponding controls. Furthermore, the use of a double-tagged LC3 construct (pmCherry-EGFP-LC3b) revealed that autophagic flux in ER-α36-knockdown cells was impaired compared with that in the control cells. To further elucidate the dynamics of autophagy, CQ was used as a late-stage autophagy inhibitor to determine whether ER-α36

knockdown promotes or inhibits autophagy. CQ inhibits autophagosome degradation; therefore, when CQ treatment is administered, any observed changes in the LC3-II/LC3-I ratio represent autophagosome synthesis, whereas in the absence of CQ, they represent the combined effects of both autophagosome synthesis and degradation (33-36). In the present study, ER-α36 knockdown increased the LC3-II/LC3-I ratio in the absence of CQ, but not its presence. This suggests that ER-α36 knockdown induces the aggregation of autophagosomes due to impaired autophagosome degradation, indicating a blockade of autophagic flux.

The colocalization of LC3 with LAMP1 in the HepG2 and Huh7 cells was observed to decrease following ER-α36 knockdown in the present study, suggesting that ER-α36 downregulation disrupts autophagosome-lysosome fusion. Intact lysosomes are highly acidic, and this acidic environment is maintained by the integrity of the lysosomal membrane (37). Loss of lysosomal integrity results in elevated lysosomal pH, which can impair autophagic degradation and block autophagic flux (13,38-40). In the present study, decreased LAMP1 expression was observed following ER-α36 knockdown, suggesting a potential loss of lysosomal membrane integrity that may affect lysosomal function.

Gal-3 staining, a well-established indicator of lysosomal injury, is commonly used to assess lysosomal integrity (41). In the present study, the accumulation of Gal-3-positive puncta was observed in the liver cancer cells with ER-α36 knockdown *in vivo* and *in vitro*, further supporting a role of ER-α36 in the regulation of LMP. Together, these findings suggest that ER-α36 downregulation impairs autophagic flux and inhibits liver cancer cell proliferation.

The positioning of lysosomes within the cytoplasm has been shown to influence the rate of autophagosome-lysosome fusion, and thus regulate autophagic flux (42). For example, the knockout of biogenesis of lysosome-related organelles complex-1, which facilitates the kinesin-dependent movement of lysosomes toward the cell periphery, results in the juxtanuclear clustering of lysosomes and impairs both their encounter and fusion with autophagosomes (43). The reduction in encounters occurs due to the inability of lysosomes to move toward the peripheral cytoplasm, where autophagosomes are predominantly formed (44). Notably, the peripheral localization of lysosomes has been associated with pathological processes, including cancer cell growth, invasion and metastasis (45), whereas the accumulation of lysosomes at the juxtanuclear region is associated with reduced proteinase secretion and a reduction in the invasiveness of tumor cells (46). In the present study, ER-α36 knockdown led to the juxtanuclear clustering of lysosomes, which may impair the fusion of autophagosomes and lysosomes, thereby inhibiting autophagic flux.

The lysosome functions as a central hub for signaling networks (45). AKT signaling has been shown to regulate lysosomal positioning (29,47). Juxtanuclear clustering of lysosomes has been shown to delay the activation of mTOR complex 1 (mTORC1), mTORC2 and AKT following serum replenishment (48). By contrast, the peripheral clustering of lysosomal mTORC1 brings it closer to activated AKT, which predominantly localizes near to the plasma membrane during the recovery phase following serum starvation (42). Notably, ER-α36-mediated rapid estrogen signaling involves the AKT signaling pathway, which has been implicated in liver tumorigenesis (10). In the present study, it was found that ER-α36 downregulation induced a reduction in AKT phosphorylation and the accumulation of LAMP1 in the juxtanuclear region. In addition, the inhibition of AKT phosphorylation was found to block ER-α36-mediated effects, including its promotion of cell proliferation and induction of lysosomal dispersal to the cell periphery. A previous study reported that decreased AKT expression is associated with elevated cytosolic Ca^{2+} levels, which induce LMP and lysosomal damage (49). In the present study, the role of ER-α36-mediated rapid estrogen signaling in LMP was investigated, and the results revealed that ER-α36 downregulation reduced AKT phosphorylation and LMP *in vivo* and *in vitro*. Treatment with E2 upregulated ER-α36 and LAMP1 expression, activated AKT and increased the Lyso-Tracker staining of lysosomes in empty vector-transfected HepG2 and Huh7 cells; all these effects were attenuated by MK-2206. However, these phenomena were almost undetectable in the HepG2 and Huh7 cells with ER-α36 knockdown, suggesting AKT is involved in the lysosomal localization and LMP changes associated with ER-α36 knockdown.

However, some important issues remain to be explored. LMP often results in the translocation of lysosomal cathepsins from the lysosomal lumen to the cytoplasm, a process implicated in the regulation of various cell death pathways (16). In the present study, Lyso-Tracker Red staining and the assessment of lysosomal integrity via LAMP1 and Gal-3 puncta assays provided evidence of LMP. However, additional assays such as cathepsin release or dextran leakage assays are necessary for further confirmation. Whether all these mechanisms are involved in the ER-α36-induced proliferation of liver cancer cells remains to be established.

In conclusion, the present study revealed that ER-α36 knockdown induced LMP, disrupted lysosomal membrane integrity, altered lysosomal localization and impeded autophagic activity via the inactivation of AKT. These effects may all contribute to the inhibition of liver cancer cell proliferation *in vivo* and *in vitro*. Thus, lysosomal dysfunction may be an underlying mechanism by which ER-α36 promotes liver cancer development.

Acknowledgements

Not applicable.

Funding

This study was supported by the National Natural Science Foundation of China (grant no. 81872040) and the Research Fund of Jianghan University (grant no. 2021jczx-002).

Availability of data and materials

The data generated in the present study may be requested from the corresponding author.

Authors' contributions

HuH, XW and ZWe were responsible for methodology, investigation, managing, storing and maintaining data to

ensure its reliability and availability, analysis and writing the original draft of the manuscript. AW, XF, HaH and ZWu were responsible for the methodology, investigation and the acquisition of data. XS and BS were responsible for analysis and interpretation of data, supervision, reviewing and editing the manuscript. QC, XH and HZ were responsible for the methodology, resources and the acquisition of data. YL and ZF were responsible for conceptualization, reviewing and editing the manuscript, supervision and funding acquisition. ZF and HuH confirm the authenticity of all the raw data. All authors have read and approved the final version of the manuscript.

Ethics approval and consent to participate

Al experimental procedures were performed in compliance with the National Institutes of Health guidelines for the Care and Use of Laboratory Animals and were approved by the Ethics Committee of Jianghan University (Wuhan, China; approval no. JHDXLL2024-086).

Patient consent for publication

Not applicable.

Competing interests

The authors declare that they have no competing interests.

References

1. Bray F, Laversanne M, Sung H, Ferlay J, Siegel RL, Soerjomataram I and Jemal A: Global cancer statistics 2022: GLOBOCAN estimates of incidence and mortality worldwide for 36 cancers in 185 countries. CA Cancer J Clin 74: 229-263, 2024.
2. Siegel RL, Giaquinto AN and Jemal A: Cancer statistics, 2024. CA Cancer J Clin 74: 12-49, 2024.
3. Han B, Zheng R, Zeng H, Wang S, Sun K, Chen R, Li L, Wei W and He J: Cancer incidence and mortality in China, 2022. J Natl Cancer Cent 4: 47-53, 2024.
4. Kasarinaite A, Sinton M, Saunders PTK and Hay DC: The influence of sex hormones in liver function and disease. Cells 12: 1604, 2023.
5. Iavarone M, Lampertico P, Seletti C, Donato MF, Ronchi G, del Ninno E and Colombo M: The clinical and pathogenetic significance of estrogen receptor-beta expression in chronic liver diseases and liver carcinoma. Cancer 98: 529-534, 2003.
6. Tu BB, Lin SL, Yan LY, Wang ZY, Sun QY and Qiao J: ER-α36, a novel variant of estrogen receptor α, is involved in EGFR-related carcinogenesis in endometrial cancer. Am J Obstet Gynecol 205: 227.e221-226, 2011.
7. Miceli V, Cocciadiferro L, Fregapane M, Zarcone M, Montalto G, Polito LM, Agostara B, Granata OM and Carruba G: Expression of wild-type and variant estrogen receptor alpha in liver carcinogenesis and tumor progression. OMICS 15: 313-317, 2011.
8. Su X, Xu X, Li G, Lin B, Cao J and Teng L: ER-α36: A novel biomarker and potential therapeutic target in breast cancer. Onco Targets Ther 7: 1525-1533, 2014.
9. Zhang J, Ren J, Wei J, Chong CC, Yang D, He Y, Chen GG and Lai PB: Alternative splicing of estrogen receptor alpha in hepatocellular carcinoma. BMC Cancer 16: 926, 2016.
10. You H, Meng K and Wang ZY: The ER-α36/EGFR signaling loop promotes growth of hepatocellular carcinoma cells. Steroids 134: 78-87, 2018.
11. Li G, Zhang J, Jin K, He K, Zheng Y, Xu X, Wang H, Wang H, Li Z, Yu X, *et al*: Estrogen receptor-α36 is involved in development of acquired tamoxifen resistance via regulating the growth status switch in breast cancer cells. Mol Oncol 7: 611-624, 2013.
12. Qu C, Ma J, Zhang Y, Han C, Huang L, Shen L, Li H, Wang X, Liu J, Zou W, *et al*: Estrogen receptor variant ER-α36 promotes tamoxifen agonist activity in glioblastoma cells. Cancer Sci 110: 221-234, 2019.
13. Qi Z, Yang W, Xue B, Chen T, Lu X, Zhang R, Li Z, Zhao X, Zhang Y, Han F, *et al*: ROS-mediated lysosomal membrane permeabilization and autophagy inhibition regulate bleomycin-induced cellular senescence. Autophagy 20: 2000-2016, 2024.
14. Yamamoto H, Zhang S and Mizushima N: Autophagy genes in biology and disease. Nat Rev Genet 24: 382-400, 2023.
15. Gros F and Muller S: The role of lysosomes in metabolic and autoimmune diseases. Nat Rev Nephrol 19: 366-383, 2023.
16. Xiang L, Lou J, Zhao J, Geng Y, Zhang J, Wu Y, Zhao Y, Tao Z, Li Y, Qi J, *et al*: Underlying mechanism of lysosomal membrane permeabilization in CNS injury: A literature review. Mol Neurobiol 62: 626-642, 2025.
17. Nie B, Liu X, Lei C, Liang X, Zhang D and Zhang J: The role of lysosomes in airborne particulate matter-induced pulmonary toxicity. Sci Total Environ 919: 170893, 2024.
18. Eriksson I and Öllinger K: Lysosomes in cancer-at the crossroad of good and evil. Cells 13: 459, 2024.
19. Li Z, Zhang Y, Lei J and Wu Y: Autophagy in oral cancer: Promises and challenges (Review). Int J Mol Med 54: 116, 2024.
20. Ballabio A and Bonifacino JS: Lysosomes as dynamic regulators of cell and organismal homeostasis. Nat Rev Mol Cell Biol 21: 101-118, 2020.
21. Cao M, Luo X, Wu K and He X: Targeting lysosomes in human disease: From basic research to clinical applications. Signal Transduct Target Ther 6: 379, 2021.
22. Davidson SM and Vander Heiden MG: Critical functions of the lysosome in cancer biology. Annu Rev Pharmacol Toxicol 57: 481-507, 2017.
23. Weber RA, Yen FS, Nicholson SPV, Alwaseem H, Bayraktar EC, Alam M, Timson RC, La K, Abu-Remaileh M, Molina H and Birsoy K: Maintaining iron homeostasis is the key role of lysosomal acidity for cell proliferation. Mol Cell 77: 645-655.e647, 2020.
24. Wang R, Chen J, Yu H, Wei Z, Ma M, Ye X, Wu W, Chen H and Fu Z: Downregulation of estrogen receptor-α36 expression attenuates metastasis of hepatocellular carcinoma cells. Environ Toxicol 37: 1113-1123, 2022.
25. Zhang X, Deng H and Wang ZY: Estrogen activation of the mitogen-activated protein kinase is mediated by ER-α36 in ER-positive breast cancer cells. J Steroid Biochem Mol Biol 143: 434-443, 2014.
26. Wang ZY and Yin L: Estrogen receptor alpha-36 (ER-α36): A new player in human breast cancer. Mol Cell Endocrinol 418: 193-206, 2015.
27. Kendall RL and Holian A: The role of lysosomal ion channels in lysosome dysfunction. Inhal Toxicol 33: 41-54, 2021.
28. Chen Y, Zhu S, Liao T, Wang C, Han J, Yang Z, Lu X, Hu Z, Hu J, Wang X, *et al*: The HN protein of Newcastle disease virus induces cell apoptosis through the induction of lysosomal membrane permeabilization. PLoS Pathog 20: e1011981, 2024.
29. Wu B, Liu DA, Guan L, Myint PK, Chin L, Dang H, Xu Y, Ren J, Li T, Yu Z, *et al*: Stiff matrix induces exosome secretion to promote tumour growth. Nat Cell Biol 25: 415-424, 2023.
30. Li Q, Sun H, Zou J, Ge C, Yu K, Cao Y and Hong Q: Increased expression of estrogen receptor α-36 by breast cancer oncogene IKKε promotes growth of ER-negative breast cancer cells. Cell Physiol Biochem 31: 833-841, 2013.
31. Klionsky DJ, Petroni G, Amaravadi RK, Baehrecke EH, Ballabio A, Boya P, Pedro JM, Cadwell K, Cecconi F, Choi AM, *et al*: Autophagy in major human diseases. EMBO J 40: e108863, 2021.
32. Koirala M and DiPaola M: Overcoming cancer resistance: Strategies and modalities for effective treatment. Biomedicines 12: 1801, 2024.
33. Tanida I, Minematsu-Ikeguchi N, Ueno T and Kominami E: Lysosomal turnover, but not a cellular level, of endogenous LC3 is a marker for autophagy. Autophagy 1: 84-91, 2005.
34. Ju JS, Varadhachary AS, Miller SE and Weihl CC: Quantitation of 'autophagic flux' in mature skeletal muscle. Autophagy 6: 929-935, 2010.
35. Rubinsztein DC, Cuervo AM, Ravikumar B, Sarkar S, Korolchuk V, Kaushik S and Klionsky DJ: In search of an 'autophagomometer'. Autophagy 5: 585-589, 2009.
36. Ou M, Cho HY, Fu J, Thein TZ, Wang W, Swenson SD, Minea RO, Stathopoulos A, Schönthal AH, Hofman FM, *et al*: Inhibition of autophagy and induction of glioblastoma cell death by NEO214, a perillyl alcohol-rolipram conjugate. Autophagy 19: 3169-3188, 2023.

37. Nakamura S, Akayama S and Yoshimori T: Autophagy-independent function of lipidated LC3 essential for TFEB activation during the lysosomal damage responses. Autophagy 17: 581-583, 2021.
38. Chan H, Li Q, Wang X, Liu WY, Hu W, Zeng J, Xie C, Kwong TNY, Ho IHT, Liu X, *et al*: Vitamin D (3) and carbamazepine protect against Clostridioides difficile infection in mice by restoring macrophage lysosome acidification. Autophagy 18: 2050-2067, 2022.
39. Gu H, Qiu H, Yang H, Deng Z, Zhang S, Du L and He F: PRRSV utilizes MALT1-regulated autophagy flux to switch virus spread and reserve. Autophagy 20: 2697-2718, 2024.
40. Zhang J, Zeng W, Han Y, Lee WR, Liou J and Jiang Y: Lysosomal LAMP proteins regulate lysosomal pH by direct inhibition of the TMEM175 channel. Mol Cell 83: 2524-2539.e2527, 2023.
41. Tanaka T, Warner BM, Michael DG, Nakamura H, Odani T, Yin H, Atsumi T, Noguchi M and Chiorini JA: LAMP3 inhibits autophagy and contributes to cell death by lysosomal membrane permeabilization. Autophagy 18: 1629-1647, 2022.
42. Korolchuk VI, Saiki S, Lichtenberg M, Siddiqi FH, Roberts EA, Imarisio S, Jahreiss L, Sarkar S, Futter M, Menzies FM, *et al*: Lysosomal positioning coordinates cellular nutrient responses. Nat Cell Biol 13: 453-460, 2011.
43. Jia R, Guardia CM, Pu J, Chen Y and Bonifacino JS: BORC coordinates encounter and fusion of lysosomes with autophagosomes. Autophagy 13: 1648-1663, 2017.
44. Zhao YG, Codogno P and Zhang H: Machinery, regulation and pathophysiological implications of autophagosome maturation. Nat Rev Mol Cell Biol 22: 733-750, 2021.
45. Pu J, Schindler C, Jia R, Jarnik M, Backlund P and Bonifacino JS: BORC, a multisubunit complex that regulates lysosome positioning. Dev Cell 33: 176-188, 2015.
46. Steffan JJ, Dykes SS, Coleman DT, Adams LK, Rogers D, Carroll JL, Williams BJ and Cardelli JA: Supporting a role for the GTPase Rab7 in prostate cancer progression. PLoS One 9: e87882, 2014.
47. Palma M, Riffo E, Farias A, Coliboro-Dannich V, Espinoza-Francine L, Escalona E, Amigo R, Gutiérrez JL, Pincheira R and Castro AF: NUAK1 coordinates growth factor-dependent activation of mTORC2 and Akt signaling. Cell Biosci 13: 232, 2023.
48. Jia R and Bonifacino JS: Lysosome positioning influences mTORC2 and AKT signaling. Mol Cell 75: 26-38. e23, 2019.
49. Seo SU, Woo SM, Lee HS, Kim SH, Min KJ and Kwon TK: mTORC1/2 inhibitor and curcumin induce apoptosis through lysosomal membrane permeabilization-mediated autophagy. Oncogene 37: 5205-5220, 2018.